

Supplementary Materials for

**Strong Electron-Phonon Interaction Retarding Phonon Transport
in Superconducting Hydrogen Sulfide at High Pressures**

Jia-Yue Yang^{1,2} and Ming Hu^{3,*}

¹Institute of Mineral Engineering, Division of Material Science and Engineering, Faculty of Georesources and Materials Engineering, RWTH Aachen University, 52064 Aachen, Germany

²School of Energy and Power Engineering, Shandong University, Qingdao 266237, China

³Department of Mechanical Engineering, University of South Carolina, Columbia, SC 29208, USA

* Author to whom correspondence should be addressed. E-Mail: hu@sc.edu (M.H.)

S1. Lattice Structure

Fig. S1 shows the $Im\bar{3}m$ lattice structure of high- T_c hydrogen sulfide (H_3S) at high pressures which contains two interpenetrating SH_3 perovskite sublattices. The unit cell contains 8 atoms and the relaxed lattice constant at 200 GPa is 2.983 Å, slightly smaller than the literature value of 3.089 Å.¹ The contact distance between hydrogen atoms is approximately 1.5 Å and very short compared with the van der Waals radii sum of 2.4 Å.

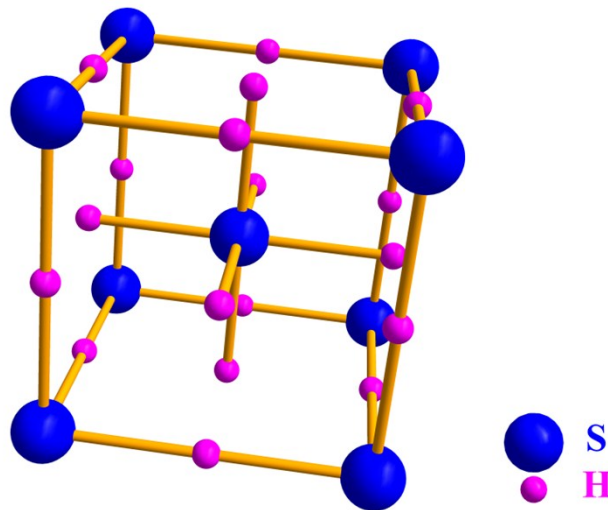


FIG. S1. The $Im\bar{3}m$ lattice structure of high- T_c H_3S at high pressures.

S2. Computational Details

We employed the Vienna *ab initio* simulation package (VASP)² using the projector augmented wave (PAW) method³ to compute harmonic as well as anharmonic interatomic force constants (IFCs) in real space and then calculate phonon dispersion relation and phonon relaxation time. The Perdew-Burke-Ernzerhof (PBE) exchange-correlation functional^{4, 5} was adopted and the energy cutoff was set as 500 eV. For the harmonic IFCs calculations, a large $3\times 3\times 3$ supercell containing 216 atoms was built and atoms were displaced from the equilibrium position by 0.02

Å. During the computations of cubic IFCs, the large $4\times 4\times 4$ supercell containing 512 atoms was chosen and a cutoff radius of 0.54 nm was introduced which is equivalent to up to the 12st nearest neighbor. After collecting the harmonic and cubic IFCs, the phonon relaxation time (τ_{ph}) and lattice thermal conductivity (κ_L) were computed with the ShengBTE package.⁶ During the calculations of τ_{ph} and κ_L , the $15\times 15\times 15$ \mathbf{q} grid was employed and the Gaussian smearing with breadth of 1 was applied to regularize the Dirac delta function to reduce computation cost but keep reasonable accuracy. To perform the electron-phonon interaction calculations, we used the all-electron full-potential linearised augmented-plane wave (FP-LAPW) ELK code.⁷ Since there exists strong anharmonicity in the hydrogen sulfide at high pressures, the supercell method was applied to include anharmonicity into phonon dispersion.⁸ The phonon calculations were performed with the q -mesh of $4\times 4\times 4$ and k -mesh of $72\times 72\times 72$.

S3. Phonon Transport by Phonon-Phonon Interaction

To explain why there exist large difference in the κ_L of H₃S at varying high pressures, the important quantities of specific heat, the averaged square group velocity and phonon relaxation time in Eq. (1) of the main text for H₃S at varying pressures are fully compared and analyzed. In Figs. S2 and S3, we do not observe a noticeable change in the specific heat and averaged square group velocity at varying pressures. However, in Fig. S4, taking the temperature of 200 K for instance, it is clearly demonstrated that the phonon relaxation time for phonons below 10 THz at 175 GPa is almost one order of magnitude smaller than that of 200 GPa, 225 GPa and 250 GPa. Further analysis on the cumulative κ_L with respect to frequency, as presented in Fig. S5, shows that the phonons below 10 THz contribute approximately 80% to the total phonon transport and are thus the major heat-carrying phonons. At 175 GPa, the T_c of H₃S is smaller than 100 K and it

is in the normal state at high temperatures as much as 200 K. However, at 200 GPa or higher, the T_c is larger than 200 K and H_3S is in the superconducting state at 200 K. Thus, we can conclude that the phonon-phonon scattering in the superconducting state is much weaker than that of normal state.

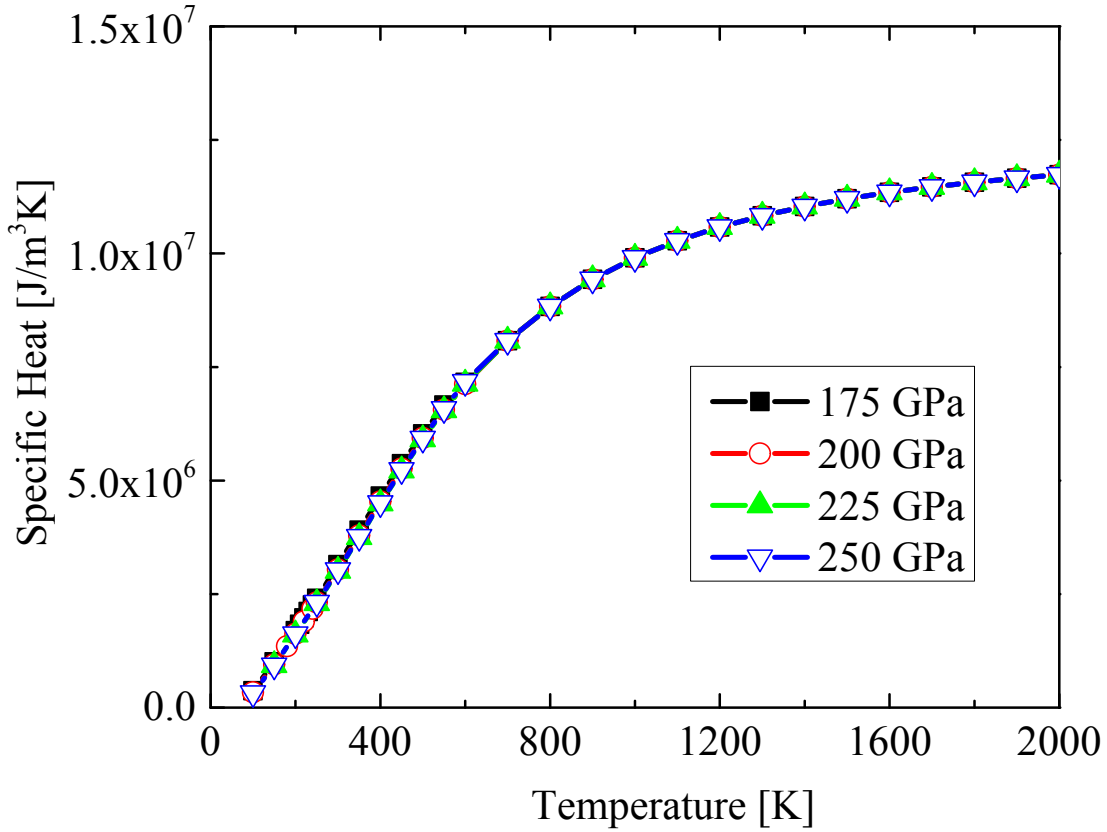


FIG. S2. The temperature-dependent specific heat of H_3S at high pressures varying from 175 GPa to 250 GPa.

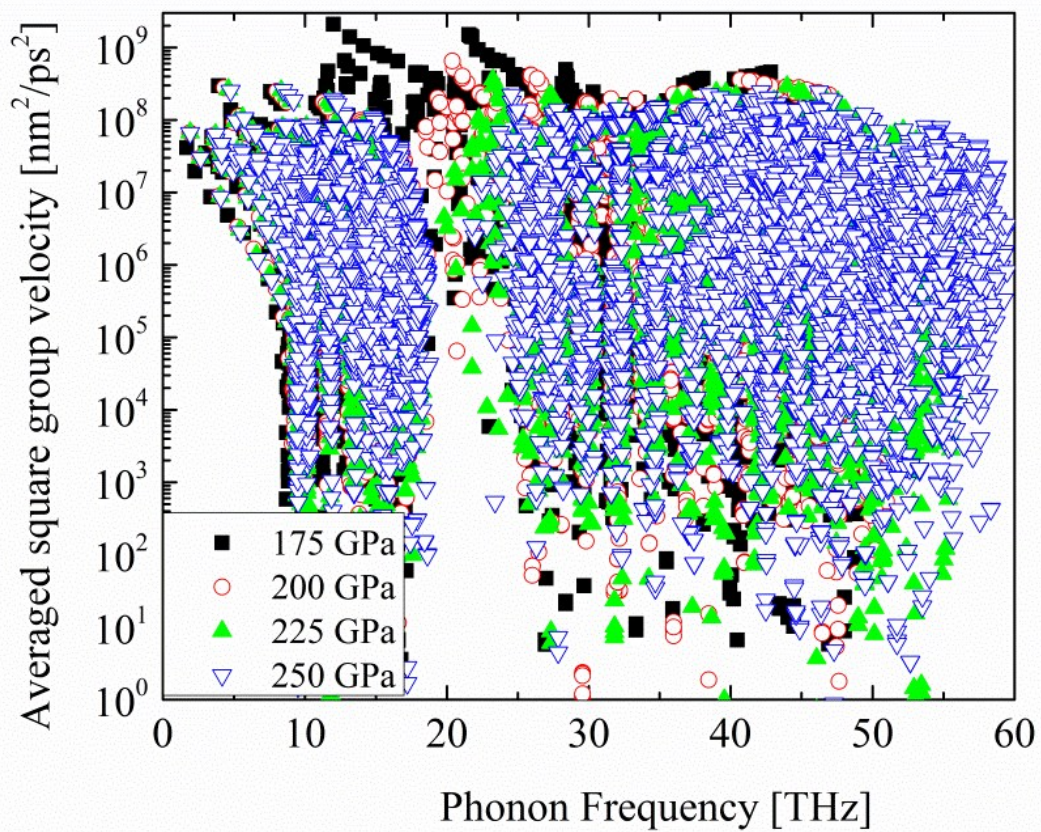


FIG. S3. The averaged square group velocity of H₃S at high pressures varying from 175 GPa to 250 GPa.

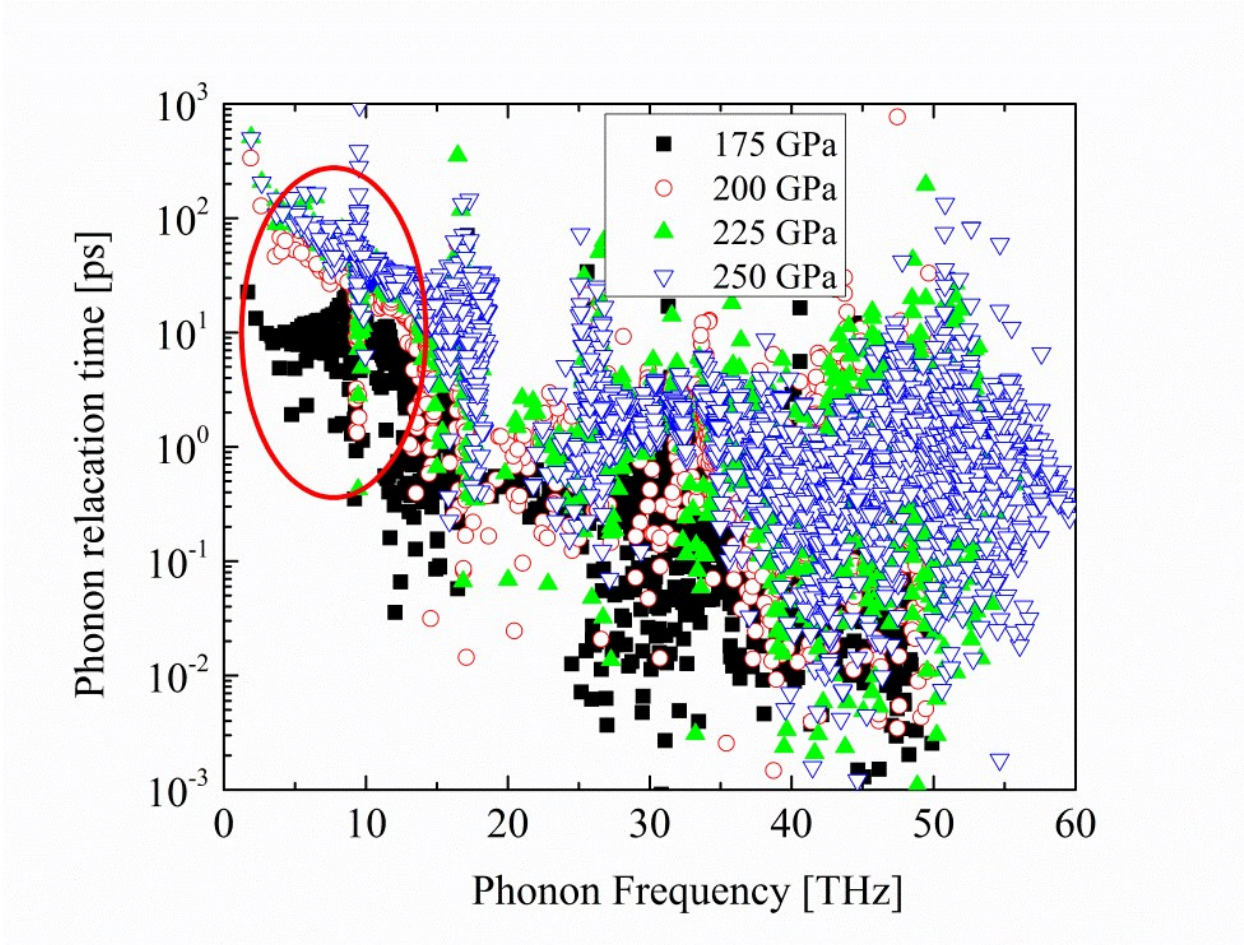


FIG. S4. The phonon relaxation time of H_3S due to only PPI at 200 K at high pressures varying from 175 GPa to 250 GPa. The red circle indicates that the relaxation time for phonons below 10 THz at 175 GPa is one order of magnitude smaller than that at higher pressures.

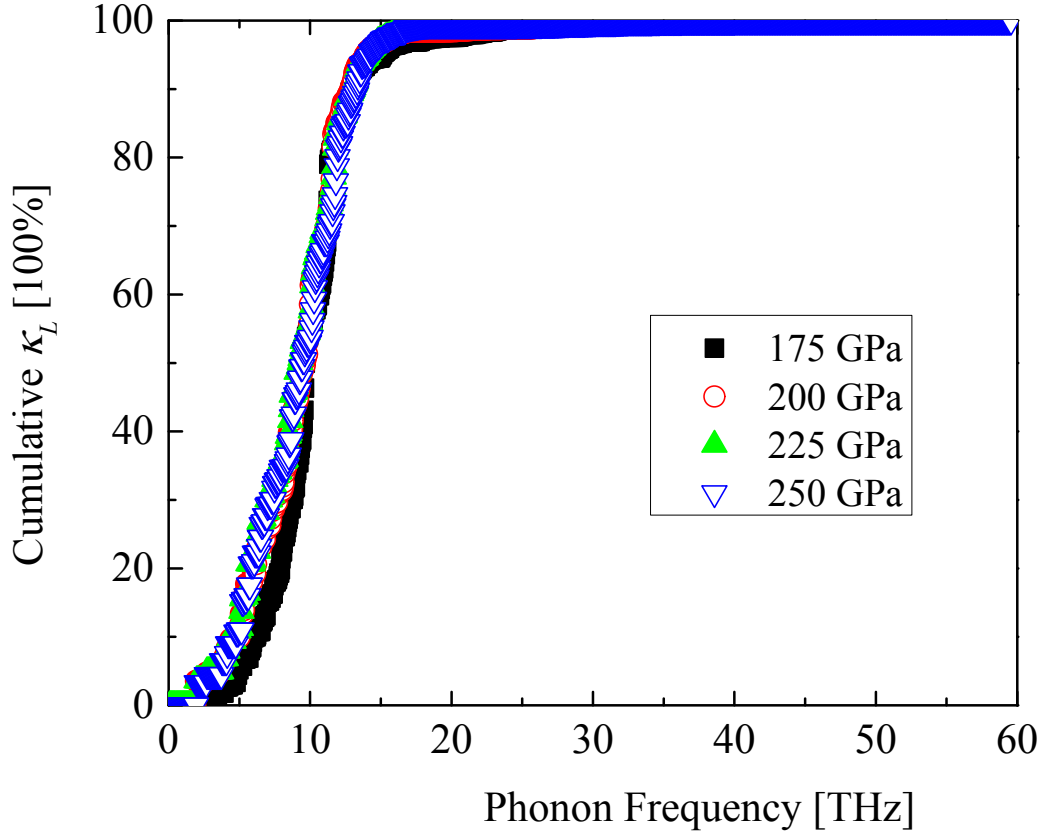


FIG. S5. The cumulative κ_L of H_3S with respect to frequency at 200 K and high pressures varying from 175 GPa to 250 GPa.

S4. Electron-Phonon Interaction under External Magnetic Field

The inclusion of external magnetic field is achieved within the framework of spin density functional theory.^{9, 10} In presence of external magnetic field $\mathbf{B}_{ext} = \nabla \times \mathbf{A}_{ext}$, the Kohn-Sham equation describing the non-interacting electrons states as^{9, 10}

$$(-1/2\nabla^2 + v_s + \mu_B \boldsymbol{\sigma} \cdot \mathbf{B}_s) \Phi_i(r) = \varepsilon_i \Phi_i(r). \quad \backslash * \text{MERGEFORMAT (S1)}$$

The noncollinear electron density ρ and magnetization density \mathbf{m} are calculated to describe the total energy $E[\rho, \mathbf{m}]$ ^{9, 10}

$$E[\rho, \mathbf{m}] = T_s[\rho, \mathbf{m}] + V_{\text{ext}}[\rho] + \mathbf{B}_{\text{ext}} \cdot \mathbf{m} + U[\rho] + E_{\text{XC}}[\rho, \mathbf{m}], \quad \text{\textbackslash*}$$

MERGEFORMAT (S2)

where T_s , V_{ext} and U is the kinetic energy, external potential and Hartree energy, respectively, μ_B is magnetic permeability and σ is the vector of Pauli matrices and. To solve this Kohn-Sham equation, a two-step variational process was proposed: (1) at the first step, the Hamiltonian containing only the scalar potential v_s is solved and the scale states serve as the basis for the second step; (2) at the second variational step, the spin-orbital coupling and magnetic terms are included. By solving those equations, the two-component spinors (Φ), noncollinear density (ρ) and magnetization density (\mathbf{m}) under external magnetic field can be obtained and further applied to compute relevantly physical quantities.

Fig. S6 shows the magnetic field dependent α^2F of superconducting hydrogen sulfide at 200 GPa. As external magnetic field is strengthened, it is demonstrated that the electron-phonon coupling strength for the high-frequency phonons slightly decreases. As is known, the strong electron-phonon coupling among high-frequency phonons is the essential condition for the high T_c of hydrogen sulfide at high pressures. Thus, the decreased electron-phonon interactions for high-frequency phonons will inevitably reduce T_c .

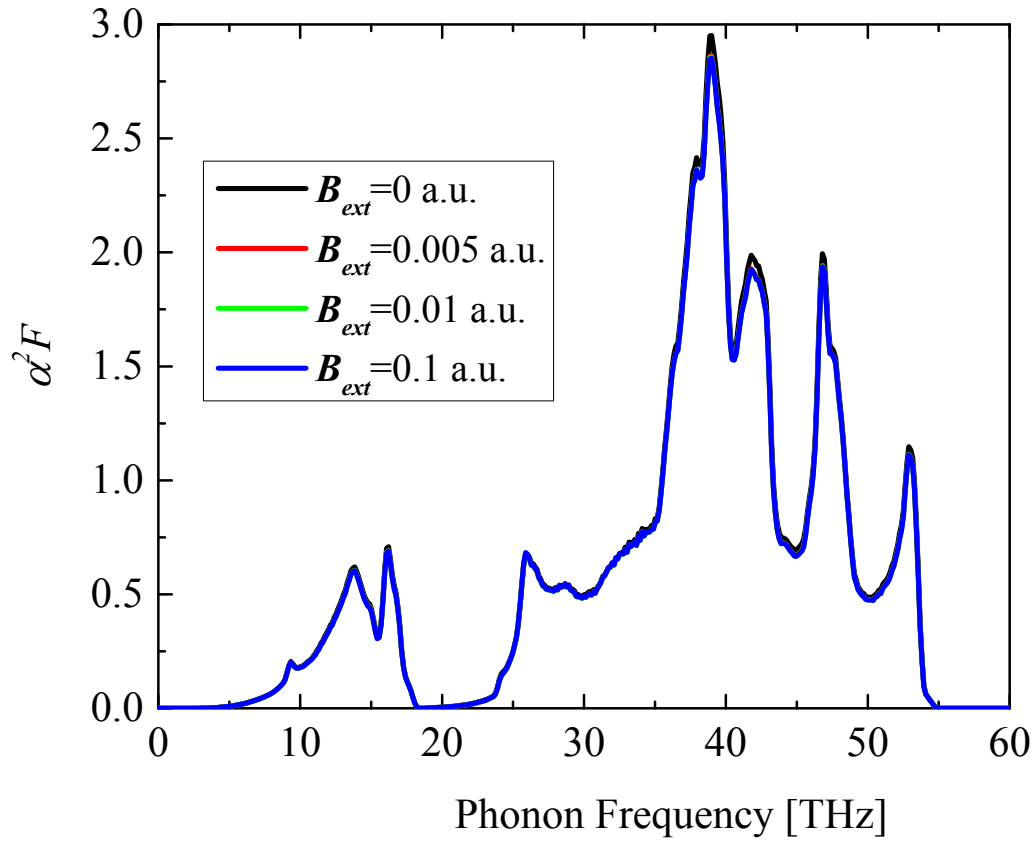


FIG. S6. The external magnetic field dependent $\alpha^2 F$ of superconducting H₃S at 200 GPa.

References

1. E. E. Gordon, K. Xu, H. Xiang, A. Bussmann-Holder, R. K. Kremer, A. Simon, J. Köhler and M. H. Whangbo, *Angew. Chem. Int. Ed.*, 2016, **55**, 3682-3684.
2. G. Kresse and J. Furthmüller, *Phys. Rev. B*, 1996, **54**, 11169-11186.
3. P. E. Blöchl, *Phys. Rev. B*, 1994, **50**, 17953-17979.
4. J. P. Perdew, *Phys. Rev. B*, 1986, **33**, 8822.
5. J. P. Perdew, K. Burke and M. Ernzerhof, *Phys. Rev. Lett.*, 1996, **77**, 3865-3868.
6. W. Li, J. Carrete, N. A. Katcho and N. Mingo, *Comp. Phys. Commun.*, 2014, **185**, 1747-1758.
7. J. K. e. a. Dewhurst, ELK FP-LAPW code, version 3.3.17 (2016); <http://elk.sourceforge.net>).
8. P. Souvatzis, T. Björkman, O. Eriksson, P. Andersson, M. Katsnelson and S. Rudin, *J. Phys.: Condens. Matt.*, 2009, **21**, 175402.
9. S. Sharma, J. K. Dewhurst, C. Ambrosch-Draxl, S. Kurth, N. Helbig, S. Pittalis, S. Shallcross, L. Nordström and E. K. U. Gross, *Phys. Rev. Lett.*, 2007, **98**, 196405.
10. S. Sharma, S. Pittalis, S. Kurth, S. Shallcross, J. K. Dewhurst and E. K. U. Gross, *Phys. Rev. B*, 2007, **76**, 100401.